Chapter 2. The mechanical strength of tetrapod-shaped granular artificial bones implanted into femoral defects in canine cadavers

Introduction

The major problem with the use of porous ceramics and granular artificial bones as bone grafts is their weak mechanical strength, which restricts their use to non-load-bearing sites (Kishimoto et al. 2006; Hirota et al. 2009; Oi et al. 2009). Although calcium phosphate cements can harden in place and provide immediate load-bearing capability with stiffness similar to that of intact bone (Ikenaga et al. 1998; Kwon et al. 2002), a study reported that the strength of the cement is still insufficient for load-bearing purposes in clinical practice (Mizobuchi et al. 2002). Therefore, strength sufficient to resist the mechanical load of the implanted bone is necessary as an ideal artificial bone.

α-TCP was useful in increasing the mechanical strength of apatite cement with larger crystals on its surface, but the mechanical strength of the apatite cement was decreased by adding β-TCP (Nakagawa et al. 2007). The higher ratio of α-TCP in the calcium phosphate cement showed the better mechanical strength for implant fixation (Yamamoto et al. 1998). Additionally, Komlev et al. reported that the cement, comprised of α-TCP and OCP had higher compressive strength.

The macrostructure design could be another important factor in the mechanical properties of the artificial bone. When the calcium phosphate ceramic could be made by mimicking the characteristics of natural bone, it showed excellent mechanical properties, and the specific structure would provide an effective way to increase the mechanical properties of porous ceramics for implantation to load-bearing bone (Zhang et al. 2007). In coastal engineering, a tetrapod is a four-legged concrete structure used as armour. The

tetrapod shape is designed to reduce displacement by mutual interlocking (Franco et al. 2000). It inspired us to apply this structure as artificial bone substitute for load-bearing site implantation. It has already been reported that the rupture strength and the elastic modulus of the Tetrabone® granule itself were significantly higher than those of β-TCP granules (Yamamoto, 2010). However, the biomechanical properties of the Tetrabone® implanted to the bone defect was still unclear.

The purpose of this chapter is to investigate the mechanical properties of the Tetrabone® implanted to the femoral defects in canine cadavers and to compare these characteristics with the β-TCP granules. Instead of the rabbit femoral defect model in chapter 1, the dog was used as a model animal. Because dog femoral defect model had been used to evaluate the osteoconductivity and biomechanical strength of the artificial bones (Frankenburg et al. 1998). Additionally, the size of the femoral defect was increased to 10 mm in diameter.

Materials and Methods

Femoral bone fragment compression

Specimen preparation

A distal femoral bone fragment including both condyles was obtained from a canine cadaver. Fourteen beagle dog cadavers (male, 10~12 kg, 1~2 years old), euthanized after the other experiments and stored in a deep freezer (-70°C) were used in this study. A cylindrical hole with 10mm in diameter was made in the distal femoral condyle in a direction perpendicular to the long axis with a power surgery drill (IMEX™ Veterinary, Inc., USA). The cortical bone was removed from the femoral condyle and a rectangular trabecular bone block with the shape of 14mm X 14mm, 8mm in depth (Fig. 2-1) was made using a sagittal saw (Osada Electronics, Tokyo, Japan). These fragments were covered with gauze rinsed with normal saline, and stored in a deep freezer (-70°C) for the mechanical study. Additionally, four other femoral bone fragments without the cylindrical hole (intact bone) were used as intact control. The frozen femoral bone fragments were thawed over 4 hours at room temperature and filled with or without granular artificial bones. They were divided into 3 groups; Tetrabone® group (N=8), β-TCP granule group (Osferion®) (N=8), and control group (N=8). In the control group, the defects were filled with PEG gel for the simulation of soft tissue. PEG (Polyethylene glycol) gel is a newly developed hydrogel by my co-worker, as a biocompatible substitute, and it has the same mechanical strength as soft tissues (Sakai, Matsunaga et al. 2008). Also in the Tetrabone® and β-TCP granule groups, granules were mixed with PEG gel before the filling procedure to make handling easier. In order to let the PEG gel harden

completely, the femoral bone fragments were covered with rinsed gauze and stored in 4°C for 24 hours before mechanical measurement.

Mechanical analysis

The femoral bone fragments were mounted on an Instron® mechanical test system (Instron-3365; Instron Corporation, Norwood, MA, USA) to determine the load-deformation changes of the specimens in vertical compression with a rate of 0.5 mm/min until fracture. All specimens were kept moist during testing. The ultimate compressive load and elastic modulus were determined from the mechanical test recordings. The elastic modulus was determined from the slope of the linear portion of the stress-strain curve. All data were expressed as a mean with standard deviation. Statistical analysis was performed by commercial software (Prism, GraphPad Software, Inc.) with one-way analysis of variance (ANOVA), where results suggested a significant difference between groups ($P < 0.05$). The data were further analyzed by Tukey's post hoc multiple comparisons test.

Defect insertion testing

Specimen preparation

A tunnel defect with a size of 10 mm in diameter, penetrating from the medial to lateral cortex of the femoral condyle, was made in the beagle dog cadavers by a power surgery drill (IMEX™ Veterinary, Inc., USA). Fifteen femoral condyles with a tunnel defect were made, covered with gauze rinsed with normal saline, and stored in a deep freezer (-70°C) for the mechanical study. These specimens were thawed over 4 hours at room temperature, filled with or without artificial bones, then divided into 3 groups; Tetrabone® group (N=6), β-

TCP granule group (Osferion®)(N=6), and control group (N=3). In the Tetrabone® and β-TCP granule groups, granules were mixed with PEG gel (Sakai et al. 2008) and formed as one block inside the tunnel defect. PEG gel was filled inside the tunnel defect in the control group. After filling, all specimens were covered with rinsed gauze and stored in 4°C for 24 hours before measurement.

Mechanical analysis

The specimens were fixed on a rheometer with bone cement, and the rod (5 mm in diameter) was vertically inserted into the exposed surface of the graft material (10mm in diameter) (Fig. 2-2). All specimens were kept moist during testing. The insertion testing was performed with the rod displacement rate of 3mm/min and the force-displacement changes were measured. In all of the experiments, loading test was performed once for each sample, because the tissue was destroyed by the measurement. The slope of the initial linear portion of the force-displacement curve was defined as compressive stiffness. All data were expressed as a mean with standard deviation. Statistical analysis was performed by commercial software (Prism, GraphPad Software, Inc.) with one-way analysis of variance (ANOVA), where results suggested a significant difference between groups ($P < 0.05$). The data were further analyzed by Tukey's post hoc multiple comparisons test.

Results

Femoral bone fragment compression

The ultimate compressive load in each group was shown in Fig. 2-3. The average value of the ultimate compressive load was 374±45 Newton in the intact bone, 188±44 Newton in the Tetrabone® group, 105±26 Newton in the β-TCP granule group, and 99±44 Newton in the control group, respectively. The ultimate compressive load of the Tetrabone® group was almost half of the intact bone and was significantly higher than that of the β-TCP granule and control groups (P<0.05). There was no significant difference in ultimate compressive load between the β-TCP granule group and the control group.

The elastic modulus in each group was shown in Fig. 2-4. The mean elastic modulus value was 1.28±0.18 Mpa in the intact bone group, 0.50±0.24 Mpa in the Tetrabone® group, 0.19±0.16 Mpa in the β-TCP granule group, and 0.20±0.17 MPa in the control group, respectively. The elastic modulus was significantly higher in the Tetrabone® group than that of the β-TCP granule and control group (P<0.05). There was no significant difference in elastic modulus between the β-TCP granule group and the control group.

Defect insertion testing

The force-displacement curve of the insertion testing was shown in Fig. 2-5. Each curve was the average value of the group. The slope of force–displacement curve was higher in the Tetrabone® group than other groups. The initial linear portion of the force–displacement curve was inside the 0.25mm of

the displacement. Therefore, the compressive stiffness was calculated inside the 0.25mm of the displacement in each group and shown in Fig. 2-6. The average value of the compressive stiffness was 14.05±6.31 N/mm in the Tetrabone® group, 3.31±1.52 N/mm in the β-TCP granule group, and 0.29±0.04 N/mm in the control group, respectively. The compressive stiffness was significantly higher in the Tetrabone® group than other groups (P<0.05). There was no significant difference in compressive stiffness between the β-TCP granule group and the control group.

Discussion

Basic mechanical measurements of bone and bone grafts include tensile, bending, compression, and torsion tests (Turner and Burr 1993; Cowin 2001). However, it is practically impossible to evaluate the granular type bone substitute by tensile, bending and torsion tests. The most adequate mechanical test for the granular bone grafts seems to be the compression test. In order to compare differences in the mechanical strength between different types of the granular bone grafts, basic biomechanical parameters of bone grafts, such as maximum strength, stiffness, and elastic modulus, were calculated and evaluated from the compression testing in many studies (Yano et al. 2000; Orr et al. 2001; Voor et al. 2004; Lunde et al. 2008). In regard to our results, the ultimate compressive load, elastic modulus and compressive stiffness were significantly higher in the Tetrabone® group than the β-TCP granule and control groups. However, there was no significant difference in these biomechanical parameters between the β-TCP granule group and the control group. These results indicate that Tetrabone® itself is mechanically stronger than the β-TCP granules due to the interlocking effects between each granules and between bone and granules.

Femoral bone compression test was performed to evaluate the whole strength of bone and implant combination, which could mimic *in vivo* situation. In the femoral bone compression, the difference in mechanical strength between the Tetrabone® and β-TCP granule was significant but not so large when compared with the data in defect insertion testing. It seemed that the trabecular bone remaining around the defect was thick enough (2mm at each side) to decrease the difference of the mechanical strength between the groups (Orr et al.

2001). Femoral bone compression tests were performed for the evaluation of the biomechanical strength of many other artificial bone implanted into the femoral bone defect *in vivo* in previous studies (Frakenburg et al. 1998; Yano et al. 2000; Orr et al. 2001). However, from our preliminary study and previous report (Un et al. 2006), it was found that compression test using whole bone specimen could not be precise, because a large amounts of intact bone surrounding the defect was too strong mechanically and concealed the mechanical character of the bone substitute itself. In order to evaluate more accurately, I decided to trim the surrounding bone to 2 mm thick in this study. One report indicated that this trimming procedure could result in the failure of measurement due to the loss of graft (Orr et al. 2001). Therefore, this compression test with trimming does not seem to be a suitable testing for next chapter. Additionally, these methods are destructive, not allowing subsequent evaluations to confirm the data.

Similar methods to the defect insertion testing in this study were also used for the mechanical evaluation of the spine *in vivo* (Snodgrass et al. 2008) and the defect sites *in vivo* (Markel et al. 1990; Markel and Wikenheiser 1991; Guo et al. 2001; Voor et al. 2004 Wheeler et al. 2005). These methods have been used for the evaluation of compressive stiffness of the bone grafts and determination of the initial mechanical properties of the various bone grafts. Furthermore, the initial linear portion of the force–displacement curve was inside the 0.25mm of the displacement by the defect insertion testing, which suggesting the elastic region of the force-displacement curve was estimated to be 0.25 mm. We found that the specimens did not fracture at 0.25mm of displacement by this method. Therefore, after this testing, all the specimens could be used for histological

research later. These results suggested that the defect insertion testing could be a better method for analyzing the biomechanical strength than femoral bone compression, because this procedure did not require trimming and was non-destructive for the specimens. In this experiment, the subsequent histological analysis was needed to clarify the new bone formation on histology in *in vivo* experiment. Although only compressive stiffness was measured by this method, it offered useful information to explain the mechanical properties of the implanted site.

In conclusion, it was confirmed that Tetrabone® implanted in the dog defect model showed better mechanical properties than β-TCP granules. Further research on the usefulness of Tetrabone® *in vivo* should be needed.
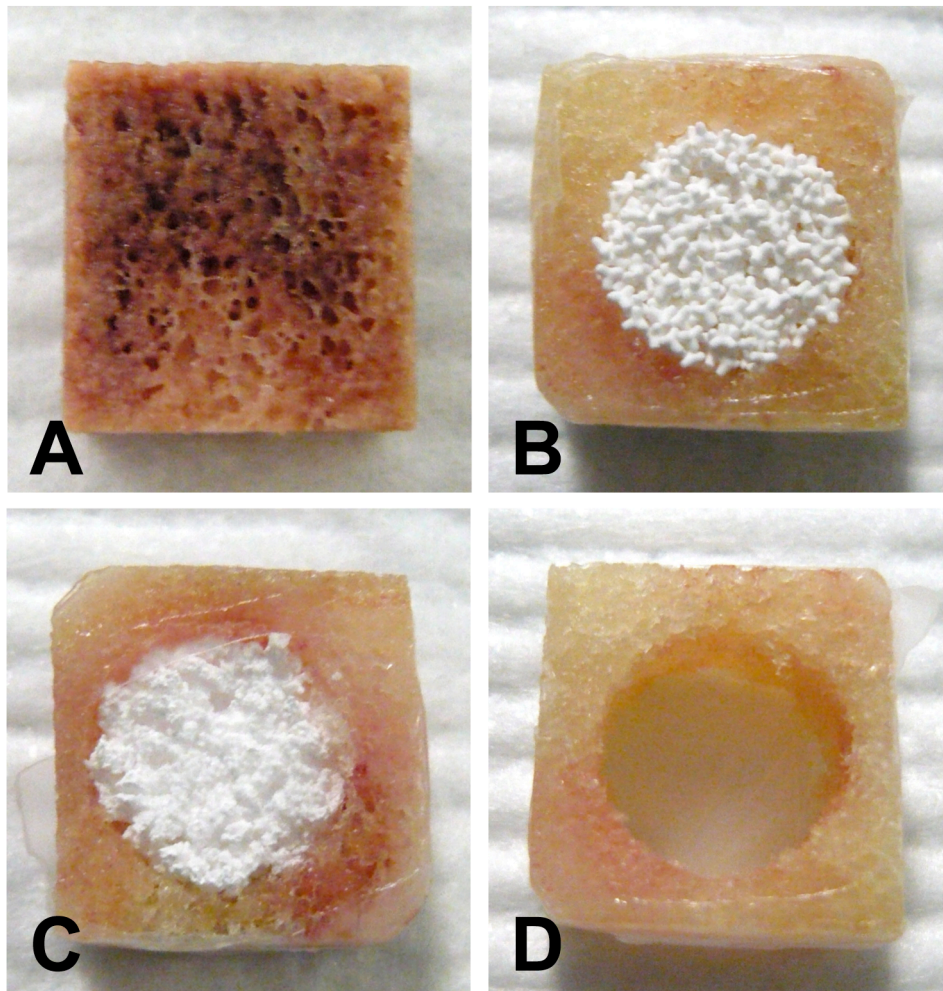
Fig.2-1 The picture of the femoral bone fragment (14mm X 14mm, 8mm in depth) in the (A) intact group, (B) Tetrabone® group, (C) β-TCP granule group, and (D) control group.
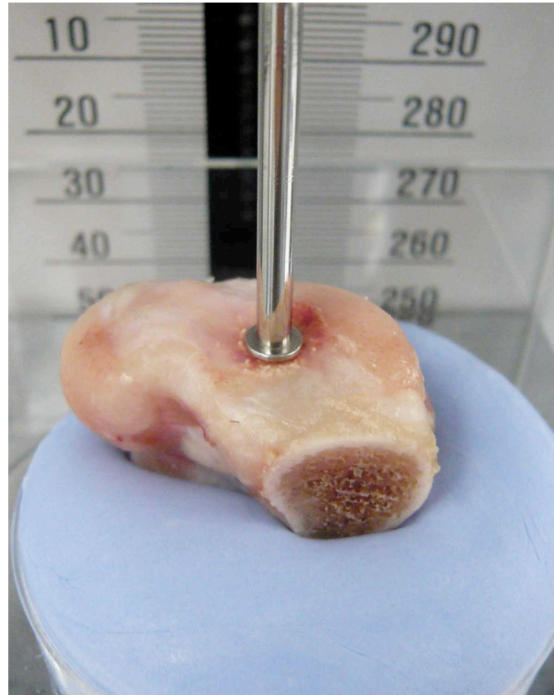
Fig.2-2 The picture of the defect insertion testing. A rod with 5mm in diameter
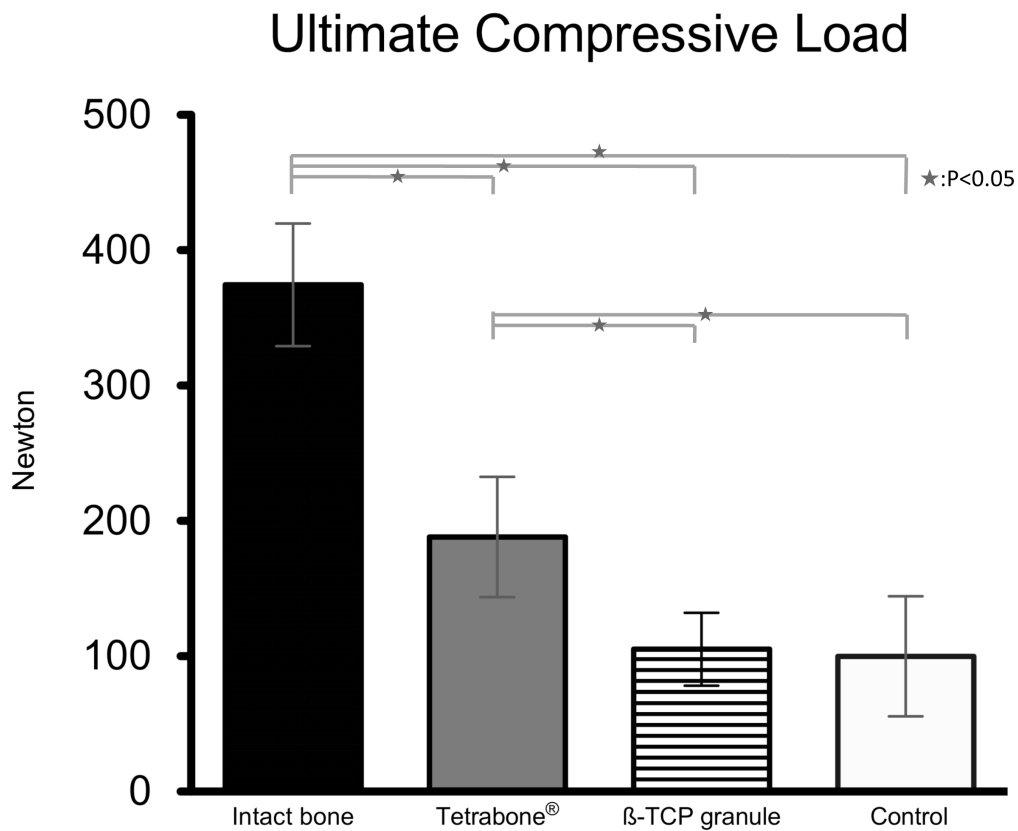
was vertically inserted to the opening of the defect.

Fig.2-3 The ultimate compressive load in each group of femoral bone fragment compression. Values are shown as mean ± SD. The ultimate compressive load of the Tetrabone® group was significantly higher than those of the β-TCP granule and control groups. There was no significant difference between the β-TCP granule group and the control group.
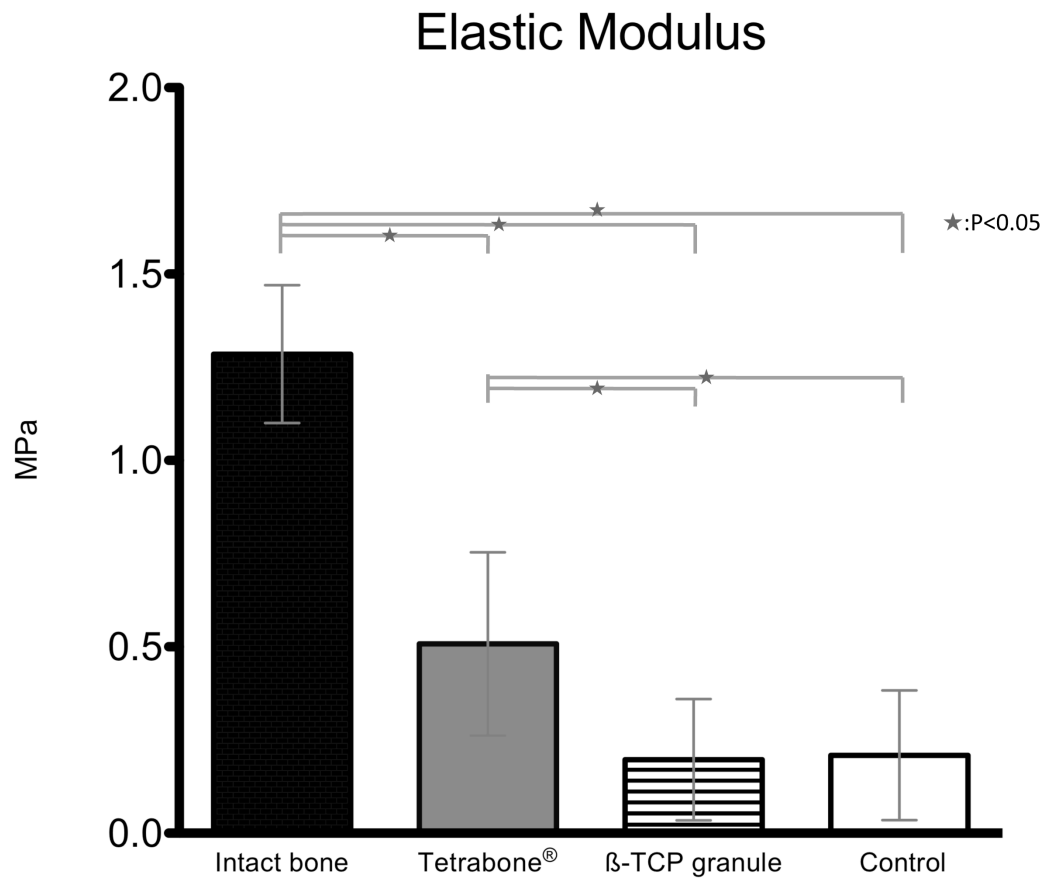
Elastic Modulus

Fig.2-4 The elastic modulus in each group of femoral bone fragment compression. Values are shown as mean ± SD. The elastic modulus was significantly higher in the Tetrabone® group than those of the β-TCP granule and control groups. There was no significant difference between the β-TCP granule group and the control group.
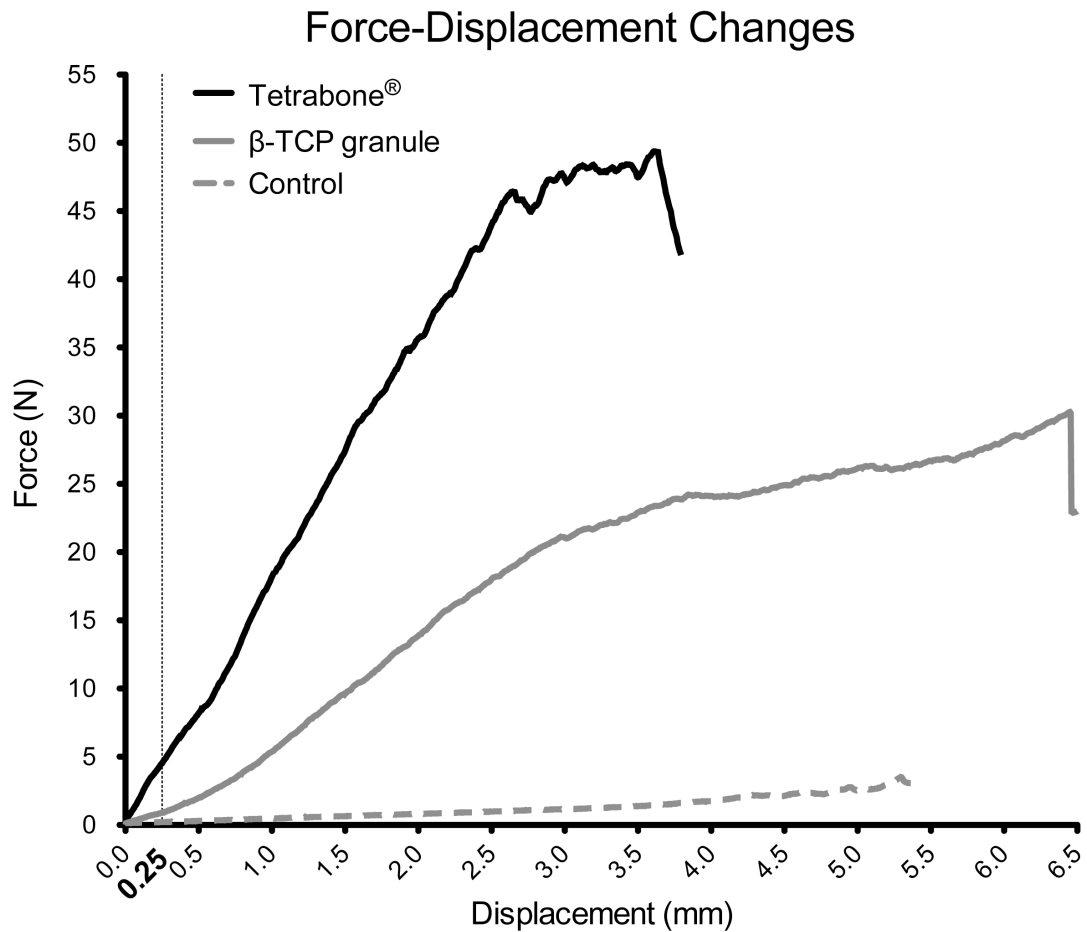
Force-Displacement Changes

Fig.2-5 The force-displacement curves in each group of defect insertion test. Values are shown as mean. The slope of force–displacement curve was higher in the Tetrabone® group than other groups. The initial linear region of the force–displacement curve inside the 0.25mm of the displacement was used to calculate the compressive stiffness.
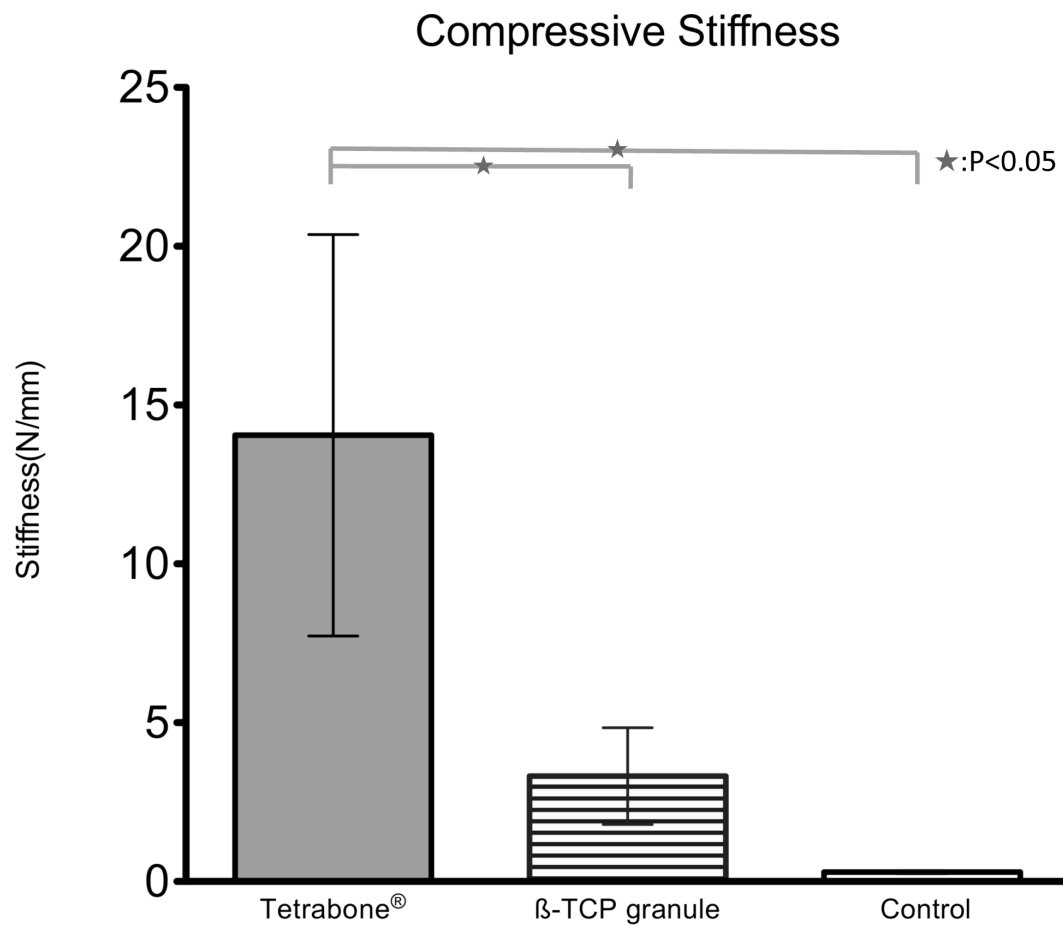
Fig.2-6 The compressive stiffness in each group of defect insertion test. Values are shown as mean ± SD. The compressive stiffness was significantly higher in the Tetrabone® group than other groups. There was no significant difference between the β-TCP granule group and the control group.

Chapter 3. New bone formation and change in mechanical strength in canine femoral defects implanted with Tetrabone®

Introduction

In chapter 2, superior mechanical properties of Tetrabone® was shown. In addition, it was expected that intergranular pores between Tetrabone® granules could work well as spaces for cell invasion. It has been well described that the porosity of biomaterials plays a significant role in adhesion, proliferation and differentiation of osteogenic cells *in vitro* and *in vivo* (Karageorgiou and Kaplan 2005; von Doernberg et al. 2006; Kasten et al. 2008). Furthermore, the interconnectivity of the pores rather than the pore size or porosity may be the primary determinant for osteoconductivity *in vivo* (Tamai et al. 2002; Yoshikawa and Tamai 2009). Therefore, the development of the artificial bone with adequate connective interpores has been expected as an ideal bone grafts (Roy et al. 2003; Simon et al. 2008). I hypothesized that aggregated Tetrabone® may have more effective intergranular pores for osteogenic cell invasion than previous substitutes. To validate this hypothesis, histological investigation in detail would be needed.

I also confirmed that Tetrabone® was resorbed very slowly with better osteoconductivity than β-TCP granules in rabbits in chapter 1. However, there were no *in vivo* studies describing the correlation between histological findings and mechanical properties of granular artificial bones made by OCP and TCP. Consequently, the change in mechanical properties after grafting *in vivo* remains unknown.

Therefore, the objective of this chapter is to investigate the *in vivo* effect of implantation with Tetrabone® to the large bone defect on new bone formation

and mechanical properties in a canine femoral defect model and to compare the effects with those of β-TCP granules.

Materials and Methods

Experimental animals

Seven male beagle dogs with the body weight of 10~12 kg and the age from 1 year to 2 years were purchased from Japan Laboratory Animals, Inc. Physical examination, complete blood count, blood chemistry analysis, and radiography for the abdomen, thorax and both hind legs were performed before implantation. All the experimental procedures using dogs were conducted under the Guidelines of the Animal Care Committee of the Graduate School of Agricultural and Life Sciences, the University of Tokyo.

Surgical procedures

The dogs were fasted for 12 hours before the implantation. Atropine sulfate (25 µg/kg) was subcutaneously injected as preanesthetic medication followed by fentanyl hydrate (5 µg/kg) intravenous injection. Propofol (6 mg/kg) was intravenously injected for anesthetic induction and anesthesia was maintained with 1.0-2.5 % isoflurane and oxygen after the tracheal intubation. Cefazolam (20mg/kg) was intravenously injected as a preoperative antibiotic. Administration of 5-20 µg/kg/hr fentanyl hydrate as an analgesic was started using a syringe pump at the time of induction of anesthesia and continued for 12 hours post-operatively.

During the surgery, ventilator was used to maintain $EtCO_2$ at about 30mmHg and fluid therapy was given with lactated Ringer's solution (10ml/kg/hr). ECG, $EtCO_2$, SpO_2, indirect blood pressure, body temperature and respiration rate were monitored during the surgery.

49

Both femurs were clipped, aseptically prepared with povidone-iodine, and draped for operation. A longitudinal incision along the femoral axis in the skin, extending through the joint capsule, was made over the medial aspect of the medial femoral condyle. The joint capsule and patella ligament were carefully elevated over the circumference of the proposed site of the defect and the trochlea was exposed. A tunnel defect with a size of 10 mm in diameter, penetrating from medial to lateral cortex, was made in the femoral condyle by a power surgery drill (IMEX™ Veterinary, Inc.). After removing bone debris and flushing with sterile saline, the tunnel defect was filled with artificial bones and both ends of the defect were sealed with fibrinogen adhesive (Bolheal®; Kaketsuken). After implantation, the joint capsule, fascia lata, and subcutaneous tissue were sutured in a continuous suture pattern with 3-0 or 4-0 polydioxanone. The skin was closed interruptedly with 3-0 nylon. The same surgical procedure was performed in the contralateral femur of the dog and all operative procedures were performed under the sterile condition. All the femoral defects were divided into 3 groups; Tetrabone® group (N=5), β-TCP granule group (Osferion®) (N=5), and control group (no treatment) (N=4).

For postoperative care, buprenorpine (15 μg/kg) and Cefazolam (20mg/kg) was injected intramuscularly twice a day for 3 days. The Robert Jones bandage was applied for bilateral hind limbs for 7 days after surgery. All dogs were observed daily for any appearance of abnormal clinical signs.

Radiography

Radiography was conducted immediately after the surgery and at 4 and 8 weeks of implantation. The lateral radiographs were taken for bilateral hind limbs, and the implants and new bone formation inside the defect were observed.

Computed tomography (CT)

The dogs were sedated using midazolam (0.3 mg/kg, IM) and medetomidine (20μg/kg, IM), and CT scanning was performed immediately after the surgery and at 4 and 8 weeks of implantation. CT data obtained were converted to transverse section of the defect using the DICOM viewer (OsiriX imaging software), and the new bone formation and the changes in the implants inside the defect were observed.

Gross evaluation

At 8 weeks of implantation, the dogs were euthanized with KCL injection under deep anesthesia with thiopental sodium at 30 mg/kg. The implants and surrounded tissues of the defects were grossly observed carefully and the femoral condyles were excised using a sagittal saw (Osada Electronics).

Micro-CT

Micro-CT scanning of the femoral condyles was performed immediately after excision as in chapter 1. The transverse sections of the defects were virtually reconstructed to observe the regenerated bone formation and artificial bones.

Out of the reconstructed 3D data, a region of interest (ROI) with a diameter of 10 mm and a height of the tunnel defect was selected for micro-CT analysis. As the same in chapter 1, non-osseous tissue volume was extracted from the whole ROI by the logic operation work and shown as the percentage area in the total ROI area.

Defect insertion testing

The defect insertion testing was performed in all samples immediately after micro-CT scanning, in the same manner as described in chapter 2. In order to avoid the destruction of the specimens, all of the experiments were stopped when the displacement reached 0.25 mm as indicated in chapter 2, and the same specimens were used for the histological study later. The compressive stiffness of each specimen was calculated and evaluated in all groups. Additionally, the compressive stiffness of the intact bone in the lateral femoral condyles were measured in 5 beagle dog cadavers to provide reference values of the defect insertion testing.

Histology

After defect insertion testing, the excised femoral condyles were fixed with neutral 10% formalin (Wako, Tokyo, Japan) for 7 days, and demineralized with Plank-Rychlo decalcifying solution (Wako, Tokyo, Japan) for 12 weeks. Decalcifying solution was changed every 3 days. After the decalcified procedure, the specimen was longitudinally bisected in the middle of the trochlea into

medial and lateral halves, and the lateral half was transversely bisected in the middle of the defect by scalpel. The two cuttings could make sure that the microtome sections were made in the defect area longitudinally and transversely. Then, the decalcified tissues were dehydrated in ascending grades of ethanol, embedded in paraffin, sectioned at 7μm thickness and stained with Masson's Trichrome stain. The stained sections were examined under the light microscope (Biozero, Keyence, Osaka, Japan) for the evaluation of new bone formation.

In the transverse section of the defect, "new bone area" and "new bone distribution" were analyzed by Image J software (US National Institutes of Health, Bethesda, Maryland) as parameters of new bone formation. "New bone area", was a ratio of the new bone area to the whole defect area as used in chapter 1. Artificial bone granules and other soft tissues were not included in new bone area. "New bone distribution" was a ratio of the new bone area including granules and bone marrows to the whole defect area, which indicated the area of new bones distributed within the whole defect (Fig. 3-1).

Results

Clinical signs

All beagle dogs tolerated the bilateral involvement of the condyler defects without any complication and could bear weight on the next day after surgery. There were no clinically abnormal signs such as pain, inflammation and lameness in beagle dogs during the whole observation period.

Radiographic findings

Typical lateral radiographs of each group at each time point were shown in Fig. 3-2. In the Tetrabone® group, the defects were filled with Tetrabone® uniformly until 8 weeks of implantation. In the β-TCP granule group, the radiolucent area was observed at the center of the defect at 4weeks and 8weeks of implantation. In these two implanted groups, new bone formation was not possible to evaluate radiologically. In the control group, some new bone formation within the defect was found at 8 weeks of implantation.

CT findings

Typical CT findings of the transverse section of the defect in each group at each time point were shown in Fig. 3-3. In the Tetrabone® group, Tetrabone® granules were kept inside the defect and no change was observed until 8 weeks of implantation. In the β-TCP granule group, granules were fully loaded at post surgery, but resorbed and disappeared at the both ends and the central area of the defect at 4 and 8 weeks of implantation. In the control group, a little new

54

bone formation was found within the defect at 4 weeks and increased at 8weeks of implantation. In the Tetrabone® and β-TCP granule groups, new bone formation within the defect could not be observed.

Gross evaluation

Fig. 3-4 showed gross findings of the excised femoral condyle in each group at 8 weeks of implantation. In the Tetrabone® group, the granules were well filled inside the defect and connected to the surrounding tissue. There were no any abnormal findings around the Tetrabone® such as inflammation, granule leakage or infection. However, in the β-TCP granule group, the opening of the defect was concave-shaped and some fibrous tissues covered the surface. In the control group, the opening of the defect was also concave-shaped and was covered with many fibrous tissues.

Micro-CT scanning

Fig. 3-5 showed the typical transverse micro-CT images in each group at 8 weeks of implantation. In the Tetrabone® group, Tetrabones were well connected with new bones and were maintained within the defect until 8 weeks of implantation. In the β-TCP granule group, granules were resorbed and disappeared at the both ends and the central area of the defect as shown on radiography. A little new bone tissue was observed in the surrounding area of the defect. In the control group, some new bones were found in the defect. However, cortical bone regeneration was not found, unlike the rabbit model in chapter 1.

Fig. 3-6 showed the non-osseous tissue volume on the micro-CT images of the Tetrabone® and β-TCP granule groups at 8 weeks of implantation. The non-osseous tissue volume was significantly higher in the β-TCP granule group (34.3±9.1 %) than that in the Tetrabone® groups (20.0±5.2 %)(P<0.05). The non-osseous tissue volume was significantly higher in the control group (90.4±3.1 %) than those in other groups (P<0.01).

Defect insertion testing

The force-displacement curve of the insertion testing at 8 weeks of implantation was shown in Fig. 3-7. Each curve was the average value of the group. The slope of force-displacement curve in the Tetrabone® group was close to the intact bone group and was clearly higher than the β-TCP granule and control groups.

The compressive stiffness at 8 weeks of implantation in each group was shown in Fig. 3-8. The average value of the compressive stiffness was 27.98±5.87 N/mm in the intact bone group, 21.58±2.43 N/mm in the Tetrabone® group, 2.90±2.14 N/mm in the β-TCP granule group, and 1.41±1.91 N/mm in the control group, respectively. The compressive stiffness at 8 weeks of implantation was significantly higher in the Tetrabone® group than the β-TCP granule and control groups (P<0.05). The compressive stiffness was significantly higher in the intact bone group than other 3 groups (P<0.05). β-TCP granule group showed no significance to the control group.

Histological observation

Fig. 3-9 showed the typical histological findings of the longitudinal and the transverse section in each group. In the Tetrabone® group, new bone formation was found in the intergranular spaces between Tetrabone® granules. The new bone tissues in the Tetrabone® group were fully distributed in the defect area. No resorption of the granules could be found in the Tetrabone® group. In the β-TCP granule group, both new bone and fibrous tissues were found in the defect. Granules were highly resorbed, leading to the appearance of empty space in the central area of the defect. The new bone tissues in the β-TCP granule group were partially distributed mainly adjacent to the original bone. In the control group, a large amount of the fibrous tissues were found in the defect and there was an empty space in the center of the defect with few new bone tissues being found near the original bone tissues.

Fig. 3-10 showed the high magnification of the transverse section of the defect. In the Tetrabone® group, new bone tissues were connected tightly and almost filled in all the intergranular spaces between Tetrabone® granules. No resorption of the granules could be found in the Tetrabone® group. In the β-TCP granule group, some new bone tissues and many fibrous tissues were found in the defect. Granules were resorbed and most of them were replaced by fibrous tissue. In the control group, new bone tissue was hardly found, and a large amount of fibrous tissues were observed.

Fig. 3-11 showed the new bone area on the histological section of each group at 8 weeks of implantation. New bone area was significantly higher in the Tetrabone® group (16.2±2.3 %) and the β-TCP granule group (15.8±3.1 %) than

in the control group (7.0±2.6 %)(P<0.05). However there was no significant difference between the Tetrabone® group and the β-TCP granule group.

Fig. 3-12 showed the new bone distribution on the histological section of each group at 8 weeks of implantation. New bone distribution was significantly higher in the Tetrabone® group (89.7±7.5 %) than in the β-TCP granule (60.9±12.4 %) and control groups (45.0±12.1 %)(P<0.05). However there was no significant difference between the β-TCP granule group and the control group.

Discussion

There were no side effects such as pain and lameness throughout the experimental period in this canine model. In addition, the toxicity or inflammatory response were not observed clinically by implantation of these artificial bone granules. Besides rabbit model used in chapter 1, the defect in the control group was not spontaneously repaired, therefore the size of the defect seemed suitable as a critical bone defect. Thus, this canine femoral defect model was considered to be a safe and suitable model to clarify the new bone regeneration by these artificial bone granules.

In this chapter, it was the main purpose to evaluate the mechanical characteristics of Tetrabone® after implantation *in vivo*. As shown in Fig. 3-7 and Fig. 3-8, compressive stiffness of Tetrabone® at 8 weeks was significantly higher than that of β-TCP granule, indicating that Tetrabone® could work *in vivo* as mechanically stronger bone graft. However, from the histological findings, new bone area showed no significant difference between Tetrabone® and β-TCP granule groups. In chapter 1 of the rabbit model, new bone area at 4 weeks showed no significant difference between Tetrabone® and β-TCP granule groups, too. It was suggested that, there is no difference in the amount of the new bone formation between Tetrabone® and β-TCP granules at early phase after this implantation. Then, it could be speculated that some other factors than new bone amount would contribute to the superior mechanical strength of Tetrabone® *in vivo*. There would be 2 important factors, including ideal resorption rate and good interconnectivity of Tetrabone®.

On radiology and histology, β-TCP granules were resorbed with a significantly shorter period than Tetrabone® granules in this study, resulting in more non-osseous tissue volume than in the Tetrabone® group. In the previous studies, these findings were also reported. β-TCP showed earlier resorption independent of bone formation and resulting in insufficient bone regeneration (Merten et al. 2001; Kurashina et al. 2002; Hirota et al. 2009). In the rabbit model in chapter 1, β-TCP granules were disappeared in the early phase of implantation. Base on these results, it is suggested that disappearance of β-TCP due to rapid resorption in the earlier phase may cause the weakened mechanical strength.

It was reported that the interconnectivity of the pores may primarily dominate the osteoconductivity *in vivo* (Tamai et al. 2002; Yoshikawa and Tamai 2009). An ideal bone graft should have adequate connective interpores (Roy et al. 2003; Simon et al. 2008). Tetrabone® granules may have suitable interpores with less than 600 μm (unpublished data) which make a dense interpore network between the granules. On the contrary, as β-TCP granules have irregular size and shape, the intergranular pores were irregular in size and shape and can make only sparse interconnectivity between the granules. This may cause that more new bone tissues could invade into the intergranular pores of Tetrabone® in the early phase of implantation, and new bone tissues were fully distributed inside the defect. In addition, new bone tissues were mostly distributed around the periphery than the center of the defect due to less interconnectivity to the central area in β-TCP granules (Wheeler et al. 2005). It is suggested that Tetrabone® had better osteoconductivity than β-TCP granules *in vivo*.

In chapter 2, superior mechanical properties were observed at the defect by implantation of Tetrabone® *in vitro*. In this chapter, the compressive stiffness of the defect in the Tetrabone® group was maintained almost 80% of the intact bone after 8 weeks of implantation and was significantly higher than that in the β-TCP granule group. The main cause of high mechanical strength was that of Tetrabone® itself, however the new bone regenerated around the granules must also contribute. In the magnified histology section, new bone tissues were fulfilled in the intergranular pores between granules in the Tetrabone® group. However, in the β-TCP granule group, granules were almost resorbed and most of them were replaced by fibrous tissues. Therefore the opening of the defect was concave, suggesting the weaker mechanical strength of the defect.

Mechanical properties of the hydroxyapatite were strongly correlated to bone ingrowth in the implant after 1 year of implantation in dogs (Martin et al. 1993). It was also reported that compressive strength increased steadily in parallel to bone ingrowth in the interconnected pores (Tamai et al. 2002). These results could suggest that new bone tissues grew into the intergranular pores and bridged over the Tetrabone® granules, leading to increase compressive stiffness of the Tetrabone® at 8 weeks of implantation. In the β-TCP granule group, due to rapid resorption and many fibrous tissues within the defect, compressive stiffness was not increased at 8 weeks of implantation.

In this study, Tetrabone® could not only maintain the shape and mechanical strength of the defect but also let new bone tissue fully distributed inside the defect in a short time. Tetrabone® could be a good artificial bones for the repair of the large bone defects at load bearing site in clinical practice. Further study

would be needed to clarify the long-term effect in new bone regeneration and mechanical strength of Tetrabone®.
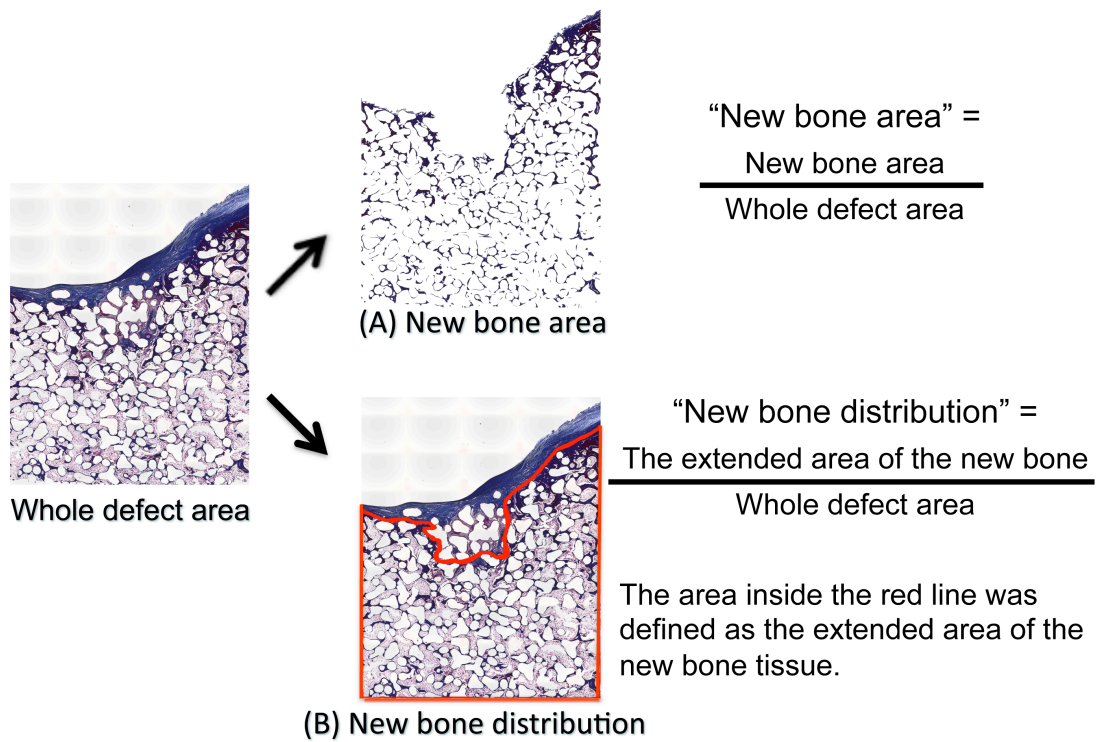
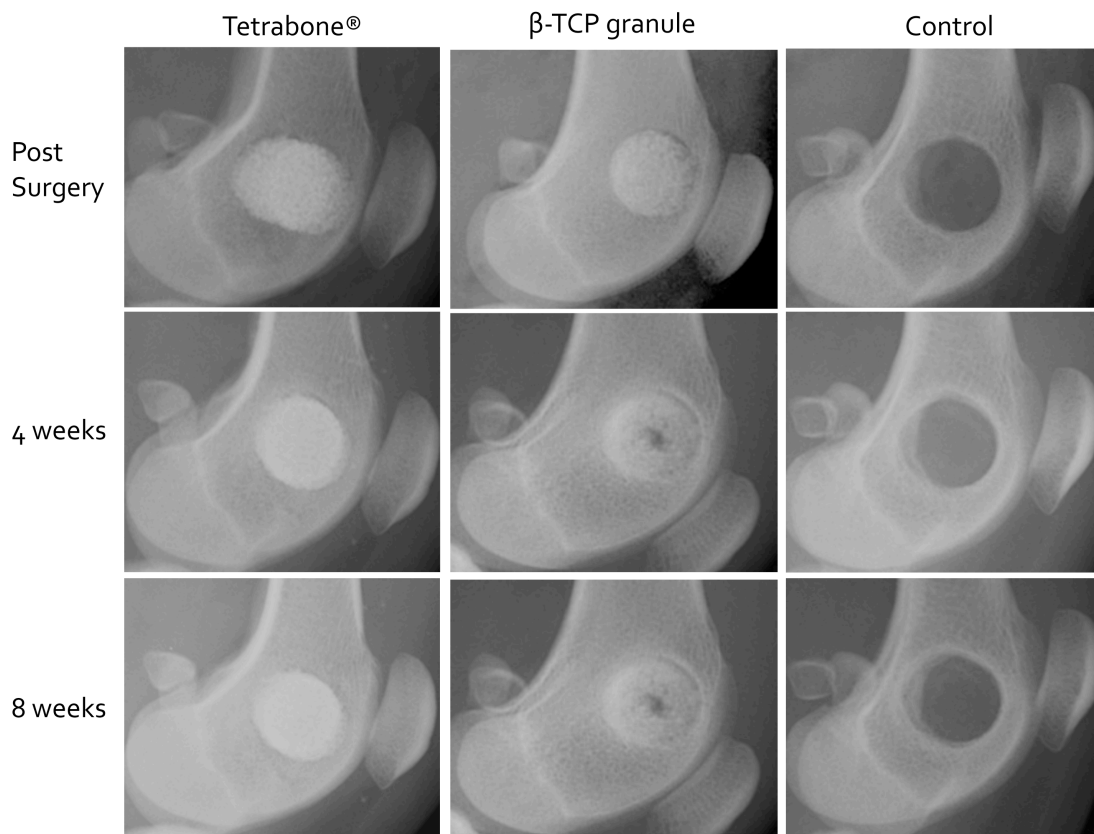**Fig.3-1** The calculation methods of (A) new bone area and (B) new bone distribution.

Fig.3-2 The typical lateral radiographic images of each group. Tetrabone® was well filled inside the defect until 8 weeks. The β-TCP granules were resorbed in the central of the defect at 4 and 8 weeks of implantation. Some new bones were found at 8 weeks of implantation in the control group.
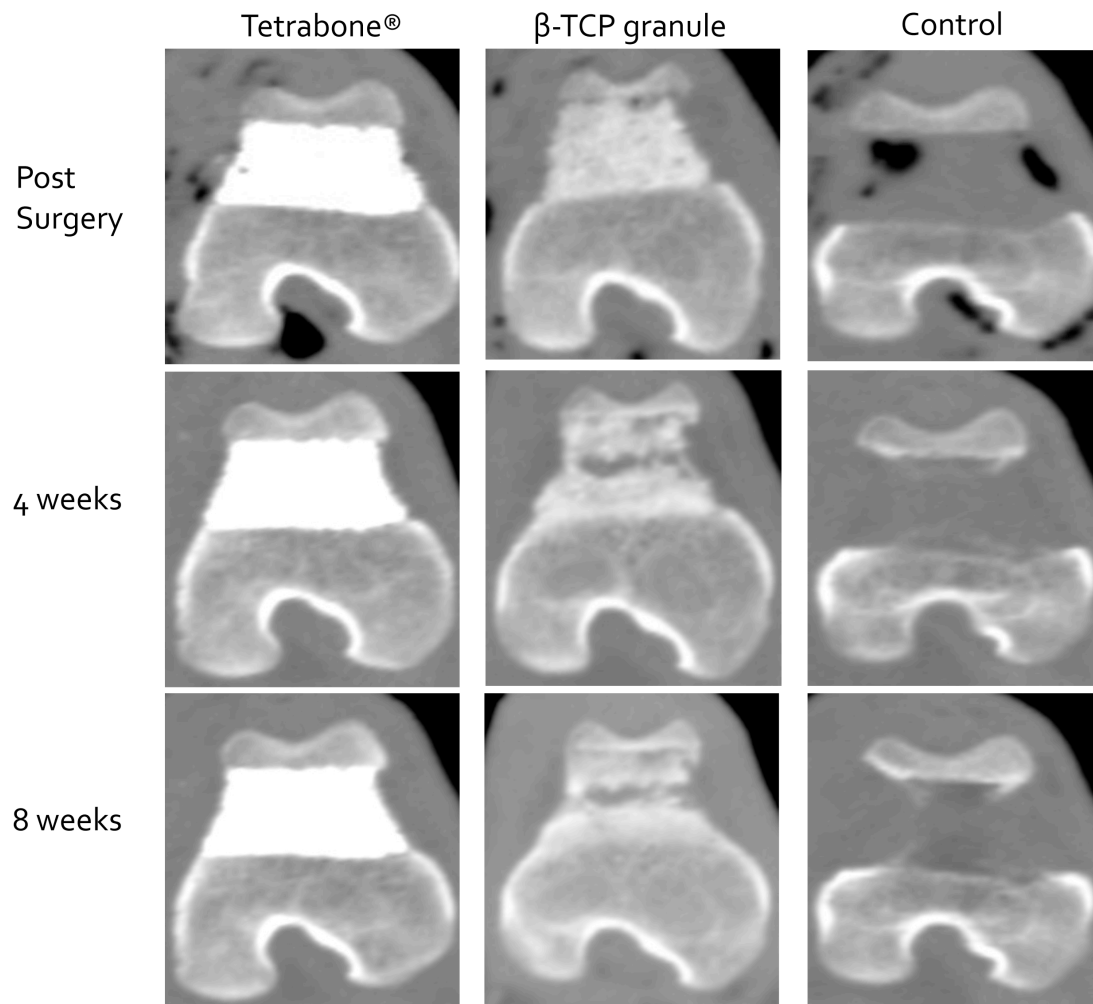
Fig.3-3 The typical transverse CT images of each group. Tetrabone[®] was well filled inside the defect until 8weeks. The β-TCP granules were resorbed at the center and both ends of the defect. Some new bones were found inside the defect and increased with time.